Supplementary information

New Pd-Fe ferrocenyl antiparasitic compounds with bioactive 8-hydroxyquinoline ligands: a comparative study with their Pt-Fe analogues

Feriannys Rivas[a], Andrea Medeiros[b,c], Cristina Quiroga[b], Diego Benítez[b], Marcelo Comini[b], Esteban Rodríguez Arce[a], Hugo Cerecetto[d], Dinorah Gambino[a]*

Table S1. Crystal data and structure refinement results for $[Pd^{II}(L)(dppf)](PF_6)$ compounds, where HL= HL1, HL3 and HL4.

	$[Pd^{II}(L1)(dppf)](PF_6)$	**$[Pd^{II}(L3)(dppf)](PF_6)$**	**$[Pd^{II}(L4)(dppf)](PF_6)$**
Empirical formula	$C_{43}H_{34}F_6FeNOP_3Pd$ [+ solvent]	$C_{43}H_{32}Cl_2F_6FeNOP_3Pd$	$C_{43}H_{32}ClF_6FeINOP_3Pd$
Formula weight	949.93	1018.75	1109.20
Temperature (K)	298 (2)	298 (2)	298 (2)
Wavelength (Å)	0.71073	1.54178	1.54178
Crystal system	Monoclinic	Monoclinic	Monoclinic
Space group	$P2_1/c$	$P2_1/c$	$P2_1/c$
Unit cell dimensions a (Å) b (Å) c (Å) β (°)	 10.6523 (4) 27.2163 (9) 16.1957 (6) 101.297 (1)	 11.9767 (5) 36.8096 (16) 9.6399 (4) 110.311 (2)	 12.1289 (2) 36.9940 (7) 9.7312 (2) 110.7210 (10)
Volume ($Å^3$)	4604.4 (3)	3985.6 (3)	4083.92 (13)
Z, density (calculated, g cm^{-1})	4, 1.3702	4, 1.698	4, 1.804
Absorption coefficient (mm^{-1})	0.865	9.501	14.607
F (000)	1912.0	2040.0	2180.0
Crystal shape/color	Rectangular prism/brown	Rectangular prism/brown	Prism/brown
Crystal size (mm^3)	0.185 × 0.222 × 0.383	0.026 × 0.095 × 0.223	0.052 × 0.062 × 0.175
ϑ-range (°) for data collection	2.9 to 25.41	3.94 to 68.40	4.78 to 68.35
Index ranges	$-12 \le h \le 12$, $-32 \le k \le 32$, $-19 \le l \le 19$	$-14 \le h \le 14$, $-44 \le k \le 44$, $-11 \le l \le 8$	$-13 \le h \le 14$, $-44 \le k \le 44$, $-11 \le l \le 9$
Reflections collected	71524	42643	30208
Independent reflections	8442	7286	7446
Observed reflections [$I>2\sigma(I)$]	7530	6753	6800
Completeness (%)	99.5	99.4	99.3
Absorption correction	multi-scan	multi-scan	multi-scan
Max. and min. transmission	0.7457 and 0.6856	0.4785 and 0.7531	0.4319 and 0.7531
Refinement method	Full-matrix least-squares	Full-matrix least-squares	Full-matrix least-squares

	on F^2	on F^2	on F^2
Data/restraints/parameters	8442/402/564	7286/225/582	7446/281/581
Goodness-of-fit on F^2	1.093	1.020	1.094
Final R indices[a] [I>2σ(I)]	R1 = 0.0376, wR2 = 0.0880	R_1 = 0.0255, wR_2 = 0.0616	R_1 = 0.0312, wR_2 = 0.0744
R indices (all data)	R1 = 0.0440, wR2 = 0.0929	R_1 = 0.0284, wR_2 = 0.0632	R_1 = 0.0351, wR_2 = 0.0763
Largest diff. peak and hole (e.Å^{-3})	0.58/-0.52	0.37/-0.35	0.59/-0.66

[a] $R_1=\Sigma||F_o|-|F_c||/\Sigma|F_o|$, $wR_2=[\Sigma w(|F_o|^2-|F_c|^2)^2/\Sigma w(|F_o|^2)^2]^{1/2}$

Table S2. Mobile phases: Gradients used in the HPLC experiment

Tiempo (min)	% A	% B
0 – 3	100	0
3 – 6	100 – 75	0 – 25
6 – 9	75 – 66	25 – 34
9 – 20	66 – 0	34 – 100
20 – 27	0	100
27 – 30	0 – 100	100 – 0

Table S3. Main FTIR bands for HL1 (8-hydroxyquinoline), HL3 (5,7-dichloro-8-quinolinol) and their [Pd(L)(dppf)](PF_6) complexes (Pd-dppf-L) (cm^{-1}).

	HL1	Pd-dppf-L1	HL3	Pd-dppf-L3
ν(O-H)	3204 (m)	-	3164 (m)	-
ν(C=N)	1508 (vs)	1501 (vs)	1498 (s)	1492 (s)
ν(C-N)	1286 (s)	1316 (m)	1275 (m)	1286 (vw)
ν(C-O)	1059 (s)	1110 (m)	1051 (w)	1116 (w)
ν: stretching; vs very strong; s strong; m medium; w weak; vw very weak				

Table S4. Main FTIR bands for HL4 (5-cloro-7-iodo-8-quinolinol), HL5 (5,7-diiodo-8-quinolinol) and their [Pd(L)(dppf)](PF_6) complexes (Pd-dppf-L) (cm^{-1}).

	HL4	**Pd-dppf-L4**	**HL5**	**Pd-dppf-L5**
ν(O-H)	3172 (m)	-	3428 (m)	-
ν(C=N)	1490 (s)	1486 (m)	1483 (s)	1480 (m)
ν(C-N)	1273 (m)	1311 (vw)	1269 (m)	1307 (vw)
ν(C-O)	1043 (w)	1098 (m)	1043 (w)	1096 (m)
ν: stretching; vs very strong; s strong; m medium; w weak; vw very weak				

Tabla S5. Main FTIR bands for HL2 (5-nitro-8-quinolinol) and [Pd(L2)(dppf)](PF_6) (cm^{-1}).

	HL2	**Pd-dppf-L2**
ν(O-H)	3172 (m)	-
ν(C=N)	1515(s)	1508 (s)
$\nu(N\text{-}O)_{as/s}$	1511 (vs) /1289 (s)	1508(s) /1291 (vs)
ν(C-N)	1273 (m)	1311 (vw)
ν(C-O)	1043 (w)	1113 (vw)
ν: stretching; vs very strong; s strong; m medium; w weak; vw very weak		

Table S6. ^{1}H NMR chemical shift values (δ, in ppm) of the ligands and the complexes in DMSO-d_6.

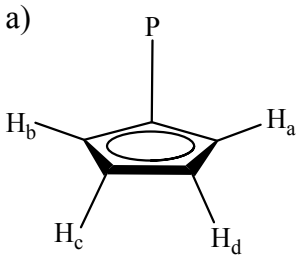

***Cp* ring (dppf)**

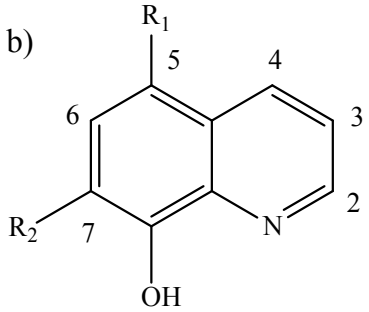

8-hydroxyquinoline

Code	R_1	R_2	
HL1	H	H	**8-hydroxyquinoline**
HL2	NO_2	H	**5-nitro-8-quinolinol**
HL3	Cl	Cl	**5,7-dichloro-8-quinolinol**
HL4	Cl	I	**5-chloro-7-iodo-8-quinolinol**
HL5	I	I	**5,7-diiodo-8-quinolinol**

H	**δ_H (multiplicity, coupling constant (Hz))(integration)**														
	HL1	**Pd-dppf-L1**	**Δδ[a]**	**HL2**	**Pd-dppf-L2**	**Δδ[a]**	**HL3**	**Pd-dppf-L3**	**Δδ[a]**	**HL4**	**Pd-dppf-L4**	**Δδ[a]**	**HL5**	**Pd-dppf-L5**	**Δδ[a]**
2	8.84 (dd, 4.1, 1.6) (1)	8.43 (d, 8.0) (1)	-0.41	9.02 (dd, 4.1, 1.2) (1)	9.31 (d, 8.9) (1)	0.29	9.00 (d, 3.3) (1)	8.55 (m)(1)	-0.45	8.97 (dd, 4.2, 1.4) (1)	8.54 (d, 8.5) (1)	-0.43	8.87 (dd, 4.1, 1.0) (1)	8.34 (br) (1)	-0.53
3	7.54 (dd, 8.3, 4.2) (1)	7.10 (m)(1)[c]	-0.44	7.89 (dd, 8.9, 4.1) (1)	7.42 (dd, 8.9, 5.0) (1)	-0.47	7.75 (dd, 8.5, 4.2) (1)	7.26 (m)(2)	-0.49	7.77 (dd, 8.6, 4.2) (1)	7.24 (m) (1)	-0.53	7.73 (dd, 8.5, 4.1) (1)	7.19 (br) (1)	-0.54
4	8.31 (dd, 8.3, 1.6) (1)	7.15 (m)(1)	-1.16	9.15 (dd, 8.9, 1.1) (1)	7.54 (m)(1)[b]	-1.61	8.50 (d, 8.5) (1)	NA	-	8.50 (dd, 8.5, 1.4) (1)	7.08 (br) (1)	-1.42	8.29 (dd, 8.6, 1.0) (1)	7.04 (br) (1)	-1.25
5	7.38 (dd,	7.10 (m)(1)[c]	-0.28	-	-	-	-	-	-	-	-		-	-	

	8.2, 1.4) (1)														
6	7.44 (m) (1)	7.36 (t, 7.8) (1)	-0.08	8.55 (d, 8.8) (1)	8.49 (d, 9.3) (1)	-0.06	7.82 (s)(1)	NA	-	8.00 (s)(1)	7.92 (s) (1)	-0.08	8.34 (s) (1)	8.20 (br) (1)	-0.14
7	7.09 (dd, 7.4, 1.5) (1)	6.30 (d, 7.7) (1)	-0.79	7.20 (d, 8.8) (1)	6.22 (d, 9.3) (1)	-0.98	-	-	-	-	-		-	-	
H_α	-	5.07 (s)(2)	1.13	-	4.73 (s)(4) 4.60 (s)(2) 4.30 (br) (2)		-	5.18 (br)(2) 4.67 (br)(4) 3.72 (br)(2)	-	-	4.72 (s)(4) 4.47 (br) (2)	-	-	4.72 (br) (4) 4.57 (br) (2) 4.29 (br) (3)	-
		3.82 (s)(2)	-0.12						-			-			-
H_β	-	4.81 (s)(2)	0.54	-		-	-		-	-		-	-		-
		4.59 (s)(2)	0.32			-			-			-			-

[a]: $\Delta\delta$: $\delta_{complex}$-δ_{ligand}
[b]: overlapped with PPh_2 protons signals
[c]: protons 3 and 5 show the same chemical shift, integrating the signal for two protons.
NA: Not assigned.
Multiplicity: s: singlet, d:doublet, dd: doublet of doublets, t: triplet, m: multiplet, br: broad.

Table S7. Retention time values for precursors [MCl_2dppf], ligands HL4 and dppf and M-dppf-L4 compounds, M = Pd(II) or Pt(II) using DMSO as solvent at t = 0.

Compounds	**RT(min)**
[Pd(L4)(dppf)](PF_6)	24.797
[Pt(L4)(dppf)](PF_6)	24.433
[$PdCl_2$(dppf)]	22.165
[$PtCl_2$(dppf)]	21.807
Dppf	27.297
HL4	22.279

Table S8. Retention time (RT) values for M-dppf-L4 compounds, M = Pd(II) or Pt(II) in DMSO/10 mM Tris-HCl buffer solution pH 7.4 (4:1).

	RT (min)	
Time	**Pd-dppf-L4**	**Pt-dppf-L4**
t = 0	24.846	24.752
t = 24 h	24.862	24.713

Table S9. Stern-Volmer constants of the Pd-dppf-L compounds and their Pt analogues for the competitive binding to {DNA-EB} adduct in 5 % DMSO/Tris HCl medium. Quenching % is included for each Pd-dppf-L compound.

Compound	K_{SV} **(M^{-1})**	**Log (K_{SV})**	**Quenching (%)**	**Compound**	K_{SV} **(M^{-1})**[a]	**Log (K_{SV})**[a]
Pd-dppf-L1	15957	4.2	60 (100 µM)	Pt-dppf-L1	2102	3.3
Pd-dppf-L2	6793	3.8	52 (110 µM)	Pt-dppf-L2	7744	3.9
Pd-dppf-L3	19525	4.3	75 (100µM)	Pt-dppf-L3	3599	3.6
Pd-dppf-L4	23471	4.4	77 (110µM)	Pt-dppf-L4	6053	3.8
Pd-dppf-L5	43942	4.6	77 (110µM)	Pt-dppf-L5	3505	3.5

[a] Data from [10]

Figures S1. FTIR spectra in KBr pellets (4000 - 400 cm^{-1}) of complexes [Pd(L)(dppf)](PF_6), where HL = HL1-HL5.

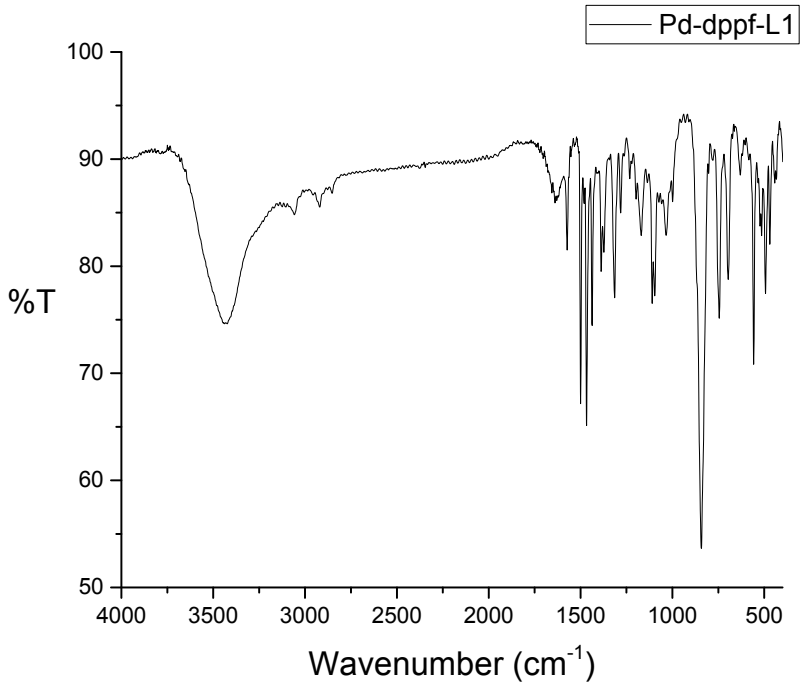

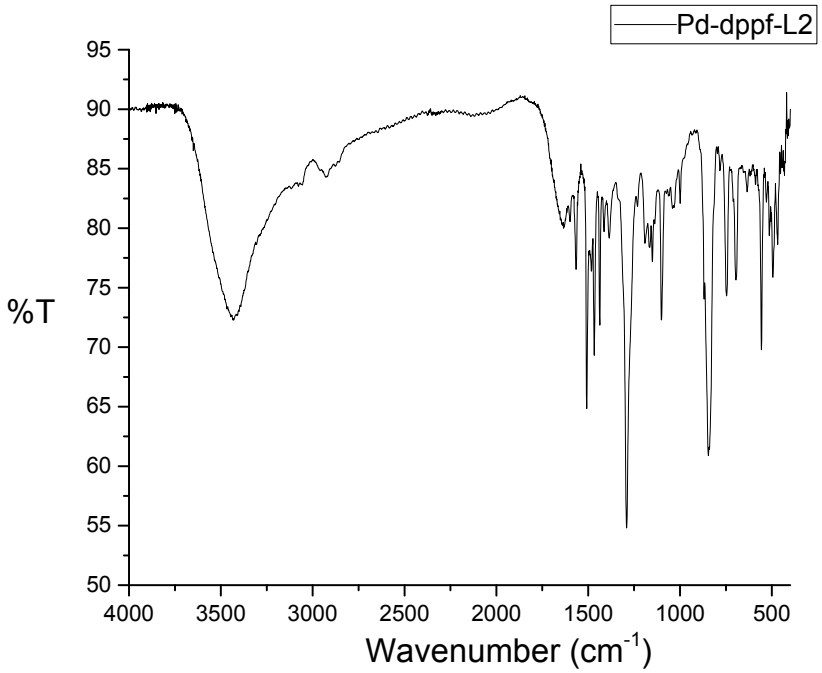

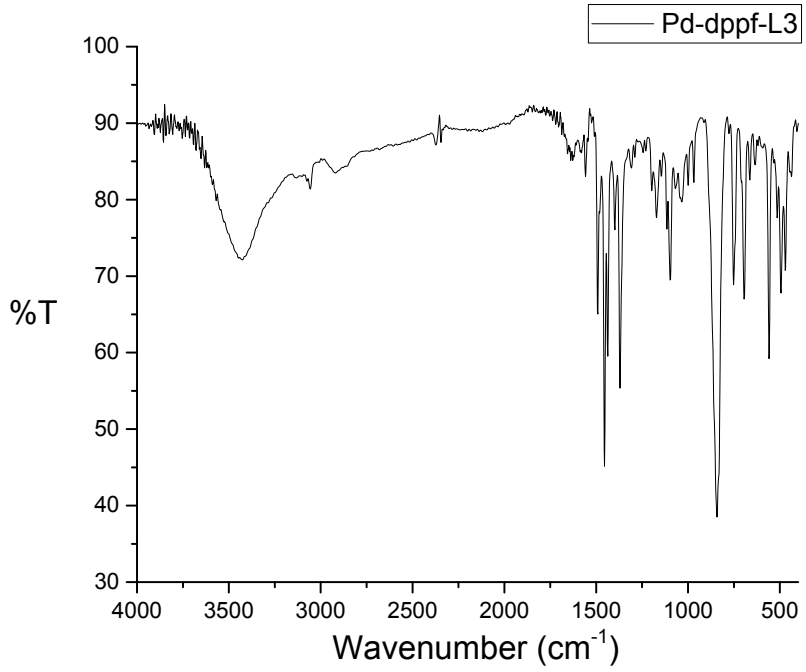
Pd-dppf-L3
100
90
80
70
60
50
40
30
%T
4000
3500
3000
2500
2000
1500
1000
500
Wavenumber (cm-1)

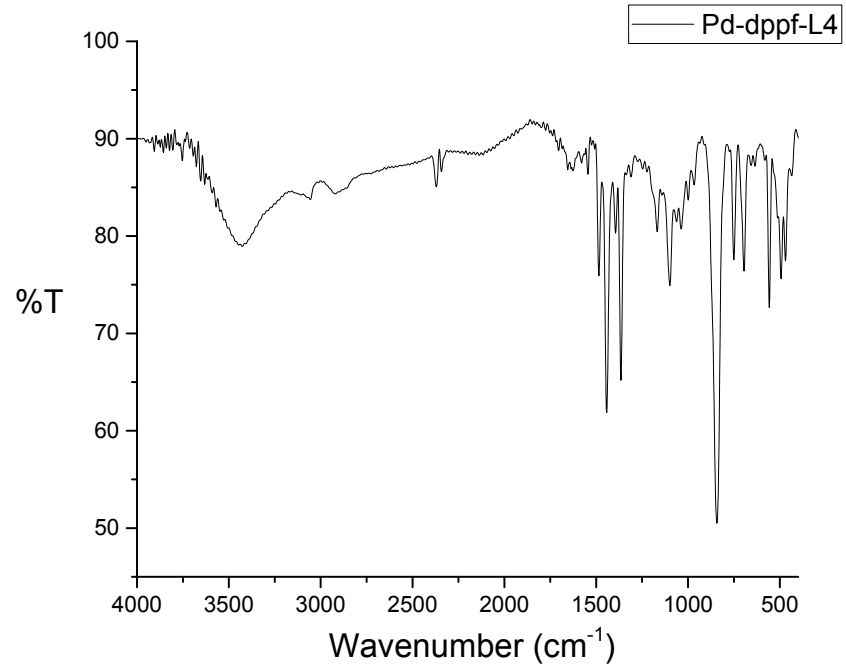
Pd-dppf-L4
100
90
80
70
60
50
%T
4000
3500
3000
2500
2000
1500
1000
500
Wavenumber (cm-1)

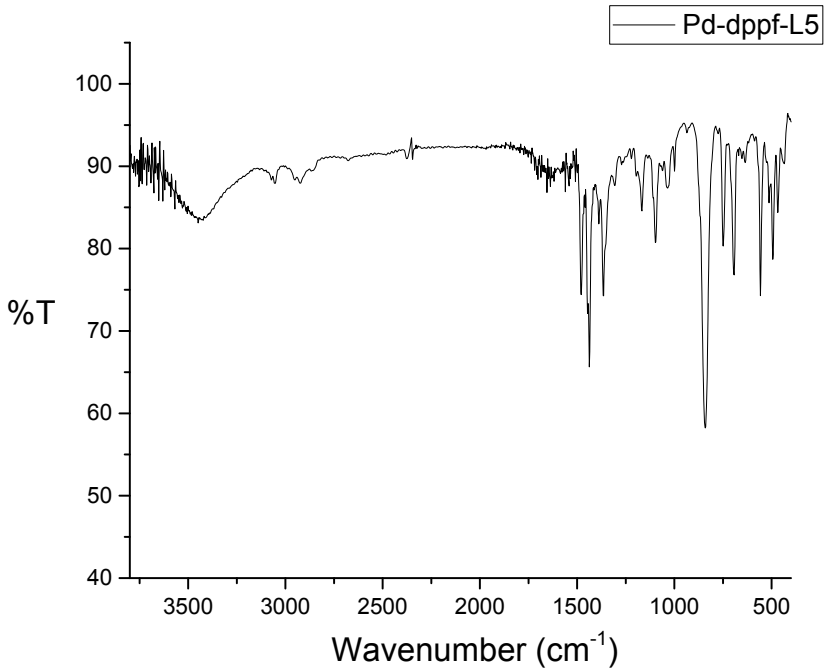
Pd-dppf-L5
%T
100
90
80
70
60
50
40
3500
3000
2500
2000
1500
1000
500
Wavenumber (cm-1)

Figures S2. ^{1}H-NMR spectra of complexes [Pd(L)(dppf)](PF_6) in DMSO-d_6 solution, where HL = HL1-HL5, compared with the respective HL ligands.

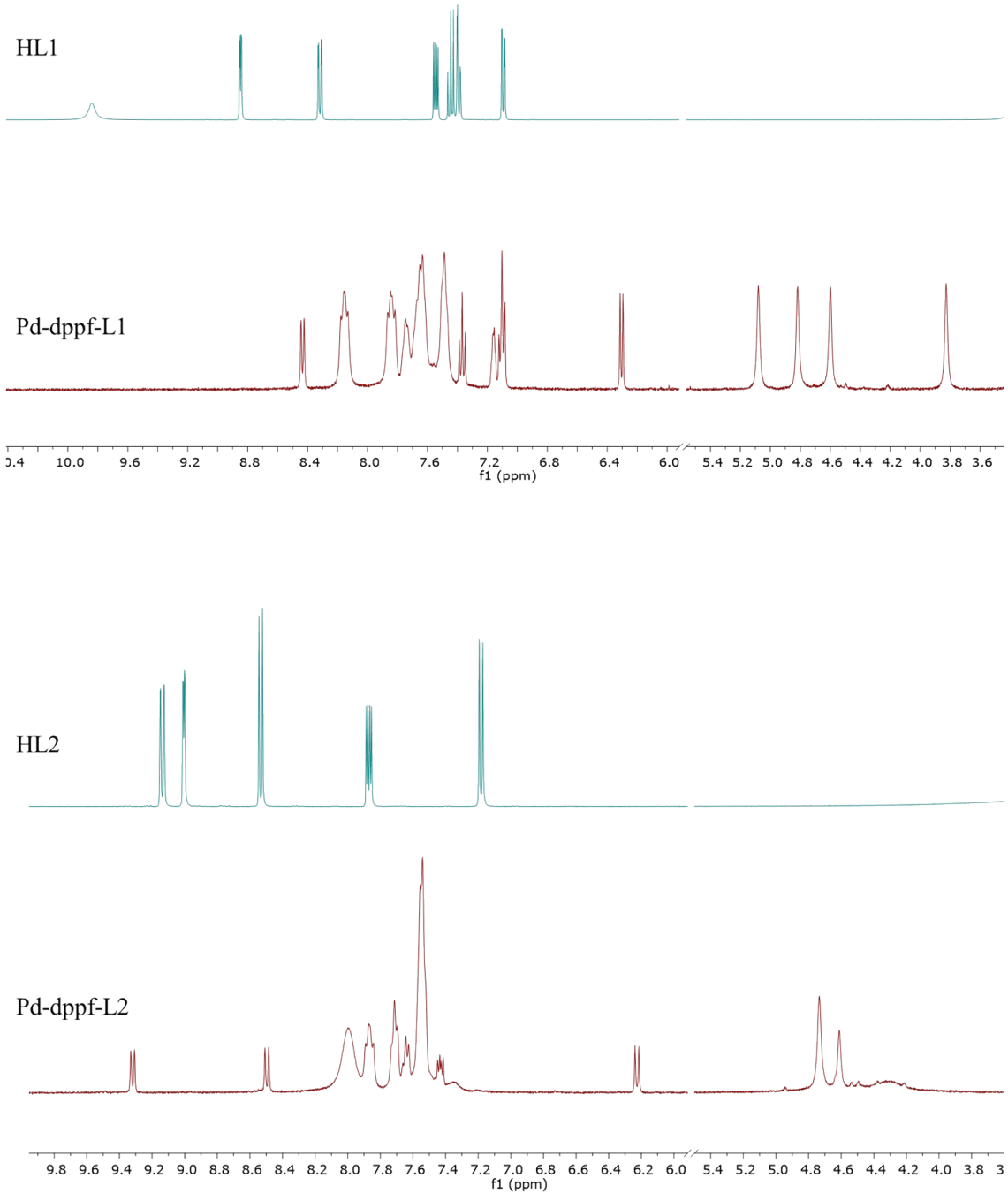

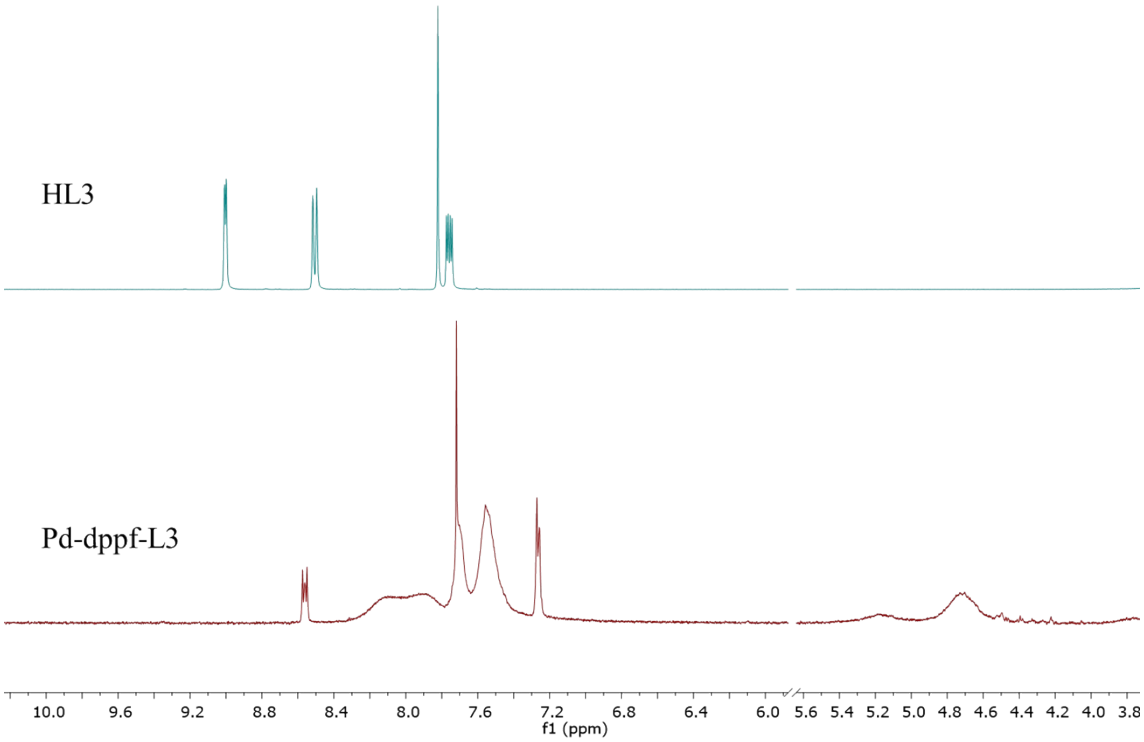
HL3
Pd-dppf-L3
10.0 9.6 9.2 8.8 8.4 8.0 7.6 7.2 6.8 6.4 6.0 5.6 5.4 5.2 5.0 4.8 4.6 4.4 4.2 4.0 3.8
f1 (ppm)

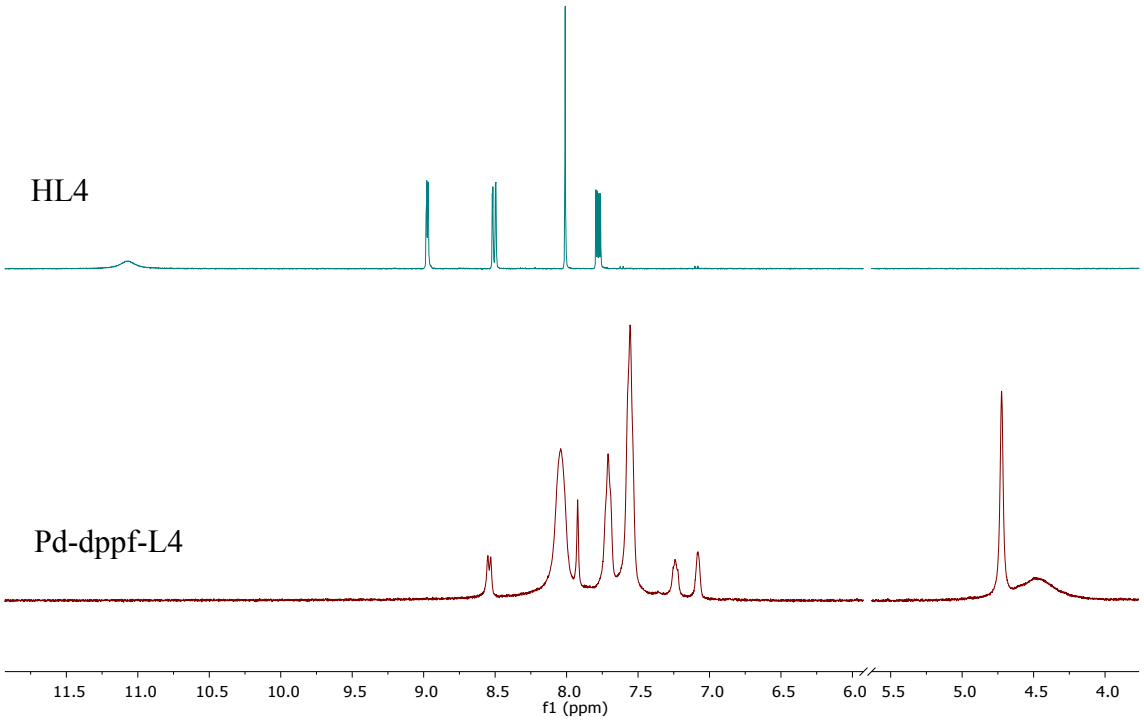
HL4
Pd-dppf-L4
11.5 11.0 10.5 10.0 9.5 9.0 8.5 8.0 7.5 7.0 6.5 6.0 5.5 5.0 4.5 4.0
f1 (ppm)

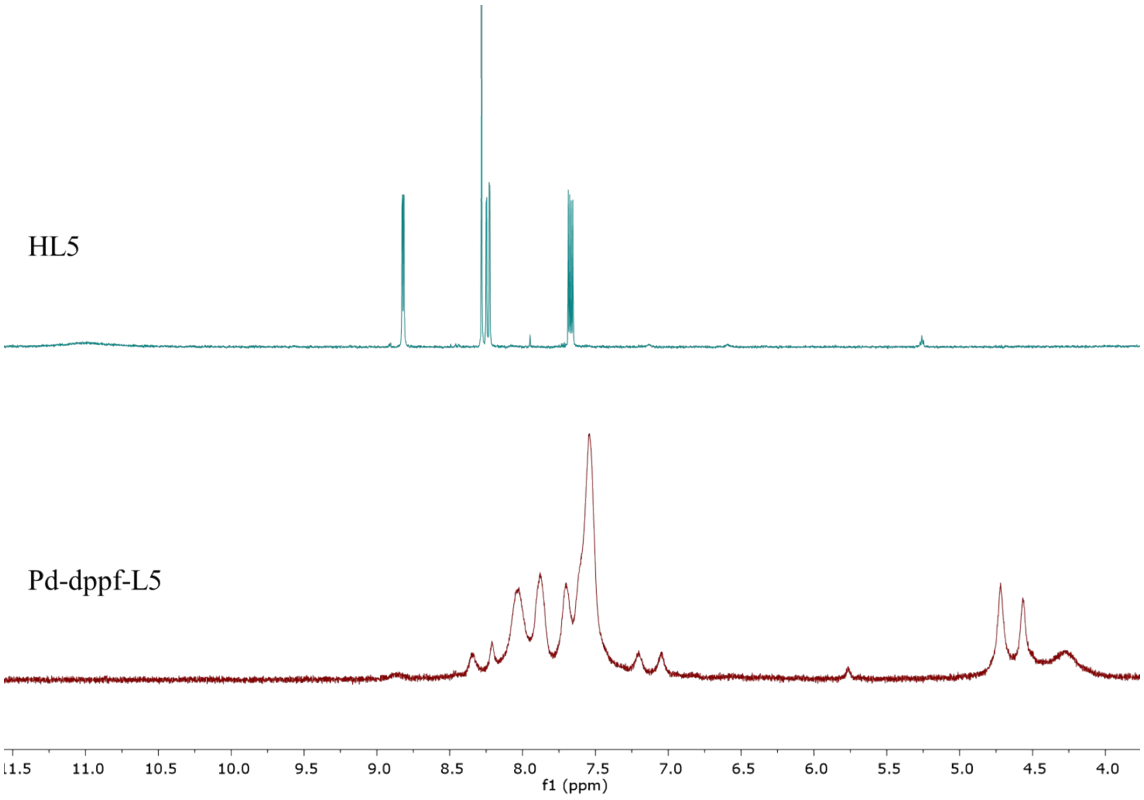
HL5
Pd-dppf-L5
11.5
11.0
10.5
10.0
9.5
9.0
8.5
8.0
7.5
7.0
6.5
6.0
5.5
5.0
4.5
4.0
f1 (ppm)

Figure S3. Chromatograms for Pd-dppf-L4 in DMSO/10 mM Tris-HCl buffer solution pH 7.4 (4:1) at t = 0 and t = 24 h.

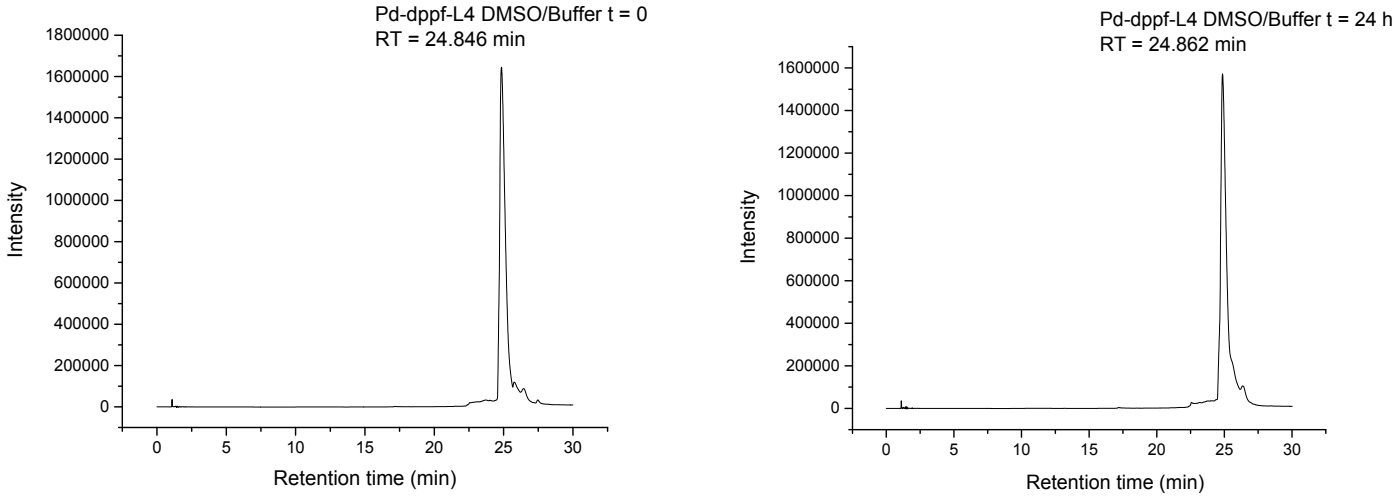

Figure S4. Chromatograms for Pt-dppf-L4 in DMSO/10 mM Tris-HCl buffer solution pH 7.4 (4:1) at t = 0 and t = 24 h

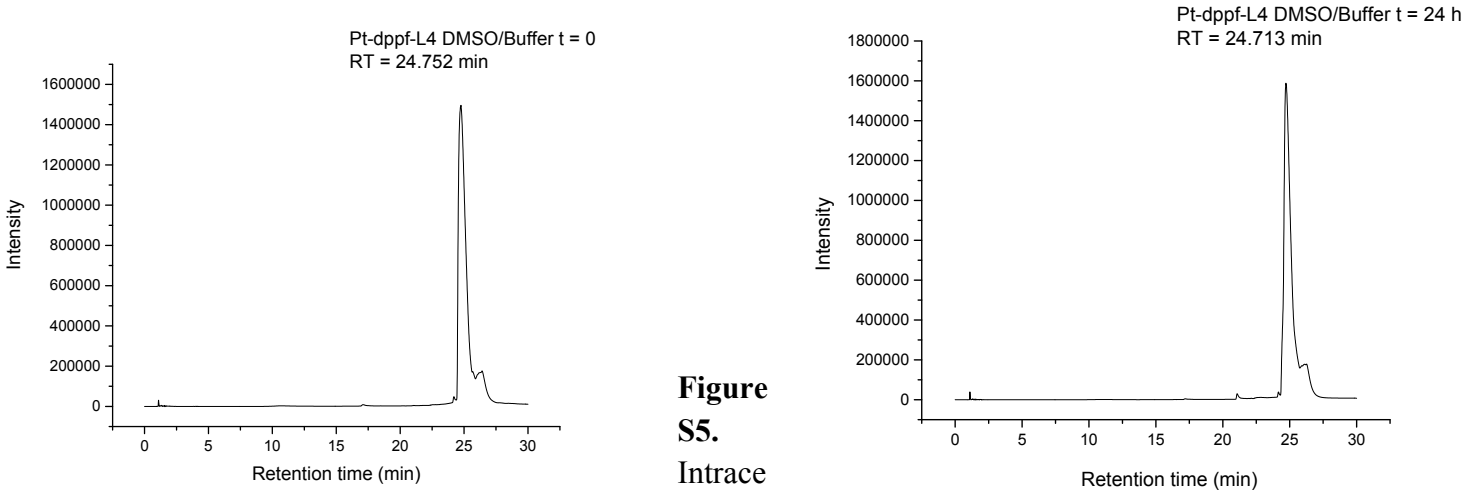

Figure S5. Intracellular redox state of bloodstream *T. brucei* treated with the compounds under study. The bloodstream form of *T. b. brucei* (5×10^5 parasites/mL) was incubated 24 h with each compound at concentrations closest to their corresponding EC_{50} values (see Table below). Thereafter, the intracellular redox state was assessed by measuring fluorescence intensity of the redox biosensor hGrx-roGFP2 expressed by the parasites. Controls included parasites treated with vehicle (DMSO 1%, v/v, red bar). For details in the protocol see section Material and Methods. The results are expressed as mean % biosensor reduction

± S.D (n = 3) with respect to the vehicle-treated parasites (100% biosensor reduction, red bar). The probability index for the compound displaying a significant oxidation of the redox biosensor is shown as inset compared to DMSO (unpaired t-Test).

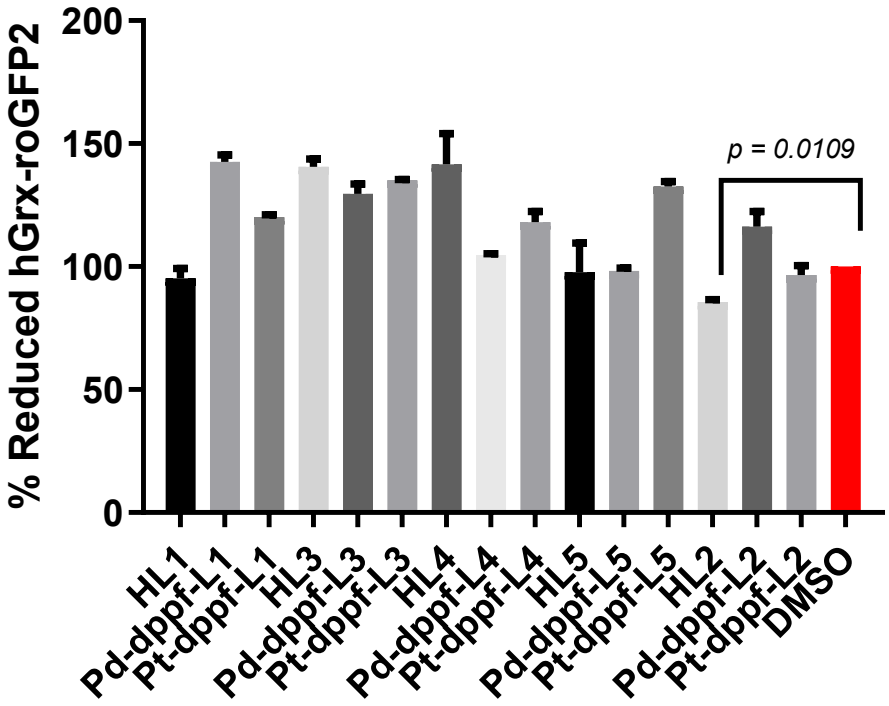

Compound	IC_{50} *T. brucei* (μM)	Concentration tested in redox assay
HL1	12.4 ± 0.8	12.5 μM
Pd-dppf-L1	0.9 ± 0.2	1 μM
Pt-dppf-L1	0.3 ± 0.1	0.25 μM
HL3	2.5 ± 0.2	2.5 μM
Pd-dppf-L3	4.5 ± 0.1	2.5 μM
Pt-dppf-L3	0.22 ± 0.01	0.25 μM
HL4	2.4 ±0.4	2.5 μM
Pd-dppf-L4	4.8 ± 0.5	2.5 μM
Pt-dppf-L4	0.14 ± 0.05	0.5 μM
HL5	3.0 ± 0.2	2.5 μM
Pd-dppf-L5	7 ± 4	0.01 μM
Pt-dppf-L5	0.22 ± 0.04	0.5 μM
HL2	0.8 ± 0.3	1 μM

Pd-dppf-L2	0.33 ± 0.09	0.25 µM
Pt-dppf-L2	0.93 ± 0.03	1 µM